Journal of Applied Polymer Science

Preparation and characterization of quartz-fiber-cloth-reinforced, polymerization-of-monomer-reactant-type polyimide substrates with a high impact strength

Xiaoli Liu,[1] Haixia Yang,[1] Jingang Liu,[1] Shiyong Yang,[1] Yanfeng Li[2]

[1]Laboratory of Advanced Polymer Materials, Institute of Chemistry, Chinese Academy of Science, Zhongguancun, Beijing 100190, People's Republic of China

[2]Department of Chemistry, Lanzhou University, Lanzhou 730000, People's Republic of China

Correspondence to: H. Yang (E-mail: yanghx@iccas.ac.cn) and S. Yang (E-mail: shiyang@iccas.ac.cn)

ABSTRACT: A series of novel quartz-fiber-cloth-reinforced polyimide substrates with low dielectric constants were successfully prepared. For this purpose, the A-stage polyimide solution was first synthesized via a polymerization-of-monomer-reactant procedure with 2,2′-bis(trifluoromethyl)benzidine and 3,3′,4,4′-oxydiphthalic anhydride as the monomers, and *cis*−5-norbornene-endo-2,3-dicarboxylic anhydride as the endcap. Then, an A-stage polyimide solution (TOPI) was impregnated with quartz-fiber cloth (QF) to afford the prepregs, which were thermally molded into the final substrate composites. The influence of the curing temperature and the resin content on the mechanical properties of the composite were examined. The composites exhibited a high glass-transition temperature over 360°C, a low and steady dielectric constant below 3.2 at a test frequency of 1–12 GHz, and a volume resistance over 1.8×10^{17} Ω cm. Meanwhile, they also showed a high mechanical strength with flexural and impact strengths in ranges 845–881 MPa and 141–155 KJ/m^2, respectively. The excellent mechanical and thermal properties and good dielectric properties indicated that they are good candidates for integrated circuit packaging substrates. © 2015 Wiley Periodicals, Inc. J. Appl. Polym. Sci. **2015**, *132*, 42358.

KEYWORDS: composites; dielectric properties; molding; polyimides; thermosets

Received 30 December 2014; accepted 12 April 2015
DOI: 10.1002/app.42358

INTRODUCTION

Low-dielectric-constant materials play an important role in the development of advanced integrated circuit (IC) manufacturing. A rigid substrate is the main requirement in high-speed signal transmission areas, such as high-end IC packaging and communication equipment in networks, because of its better dimensional stability and impact resistance compared to a flexible substrate.

A thinner substrate and higher frequency signal transmission have been required by the packaging substrate industry in recent years. Therefore, new requirements, such as a low dielectric constant and dielectric loss, good heat resistance, and low warp, have been proposed for package substrate materials. To lower the warping rate of the IC package substrate, the elastic modulus and heat resistance of the substrate material must be enhanced, and the coefficient of thermal expansion (CTE) must be reduced. Conventional rigid packaging substrates are usually built-up printed circuit boards, in which the substrate cores are made of multifunctional epoxy (FR-4) or bismaleimide–triazine resins and aromatic polyimide (PI). The high CTE and the limited thermal properties of epoxy and bismaleimide–triazine resins used in conventional packaging substrates usually result in some critical disadvantages for high-density IC packaging applications;[1] these can include delamination occurring during the manufacturing procedure. From a reliability perspective, each 10°C increase in the operating temperature results in a twofold increase in the die failure rate. Therefore, packaging materials that improve the thermal performance are very important:[2]

$$k = \frac{1+2(P_m/V_m)}{1-(P_m/V_m)} \quad (1)$$

Aromatic PI is a kind of high-performance polymer with good thermal properties,[3] a high mechanical strength, good dielectric properties,[4] and good dimensional stability. It has been widely used in flexible substrates, such as Kapton and Upilex, and has also been applied as a composite laminate matrix resin.[5,6] According to the Claslius–Mosotti equation [eq. (1)], the incorporation of atoms with low atom dielectric and substitution groups with large volumes can contribute a lower molecular polarization; thus, the material will show a low dielectric constant.[7] In addition, decreasing water absorption is another

aspect of lowering the dielectric constant for substrates. Because of the low atomic polarization of fluorine atoms and the large free volume of —CF_3 groups, the incorporation of trifluoromethyl (—CF_3) into the molecular structure of PI is a promising approach for achieving these aims. The fluorine atom can also lower the cohesive energy and surface free energy; thus, the material will exhibit a lower water absorption compared to conventional PIs. Matsuura *et al.*[8] investigated fluoride PIs and systematically studied the content of fluorine with the dielectric properties. Their research showed that with increasing fluorine, the dielectric constant of the PIs decreased. The fluorine content of PI derived from pyromellitic dianhydride and 2,2′-bis(trifluoromethyl)benzidine (TFDB) was 2.3%, and its dielectric constant was 3.5, whereas the fluorine content of PI derived from 4,4′-(hexafluoroisopropylidene) diphthalic anhydride and TFDB was 3.5%, and its dielectric constant was 2.6. Hasegawa[9] also found that PI derived from 1,2,3,4-cyclobutanetetracarboxylic dianhydride and TFDB had a lower dielectric constant (2.66), and the dielectric constant of PI derived from *trans*−1,4-cyclohexanediamine and 3,3′,4,4′-biphenyltetracarboxylic dianhydride was 2.85, although the value was estimated by the average refractive index. A lot of work has also been done on fluorinate materials,[8,10–15] but most of these works have concentrated on the film properties, and few of them have been applied to rigid-substrate packaging materials.

In the conventional electricity industry, glass-fiber cloth is used as a reinforcement to fabricate substrates.[1,16] With the rapid development of the dielectric industry, to improve the dielectric properties, various types of glass fibers have been produced to reduce the amount of impurities. E-type glass-fiber cloth was applied in Xu *et al.*'s[1] study, but the composite showed a high dielectric constant of 4.2. Quartz fiber, which has a high content of SiO_2 (≥99.9%), shows better dielectric properties and thermal properties than glass fiber. Therefore, chopped quartz fiber has been used as a reinforcement in composites. Gao *et al.*[17] used chopped quartz fiber to reinforce PI, but the CTE of PI was 50–52 ppm/°C, and the CTE of PI/QF was 43–48 ppm/°C. Their research showed that the enhancements of the mechanical properties and thermal properties through the incorporation of chopped fiber were limited. However, there has been little reported on quartz-fiber-cloth implications in the rigid-substrate packaging area. In this study, quartz-fiber cloth was applied to lower the dielectric constant and CTE.

In this study, we developed a new polymerization-of-monomer-reactant (PMR)-type PI resin[18] with a low melt viscosity, which could be conveniently produced into a multilayer laminate. To reduce the dielectric constant of PMR-type PI, TFDB with a rigid molecular structure and high fluorine content was applied. For the purpose of further reducing the dielectric constant and improving the thermal stability of the composite materials, quartz-fiber cloth was applied to prepare a multilayer composite laminate. The Cu/TOPI/QF laminate was prepared to study the adhesion properties between Cu foil and the TOPI/QF laminate; this is important for packaging substrate materials and was represented by the peel strength. The effects of the molecular weight of PI, the curing procedure, and the content of resin on the composites properties were investigated. The processability, mechanical properties, thermal stability, and dielectric properties of the QF/TOPI laminate were characterized.

EXPERIMENTAL

Materials

TFDB (Bomi Chemical Co., Beijing, China) was used as received. 3,3′,4,4′-Oxydiphthalic anhydride (ODPA; Shanghai Resin Synthesis Manufactory, Shanghai, China) was dried in a vacuum oven at 180°C for 8 h before use. Nadic anhydride (NA; Nanxiang Chemical Reagents Co., Shanghai, China) was vacuum-sublimed before use. B-Quartz cloth (QF, $SiO_2\% \geq 99.9\%$) was purchased from Feilihua Quartz, China and used as received. Copper foil (Cu), 35 μm in thickness, was obtained from Hubei Research Institute of Chemistry (China) and was used as received.

Characterization

Fourier transform infrared (FTIR) spectra were obtained on a PerkinElmer 782 FTIR spectrophotometer through the mixture of the powder samples with potassium bromide. ^{1}H-NMR was conducted on a Bruker AV-400 NMR spectrometer by the dissolution of the samples into dimethyl sulfoxide-d_6 with tetramethylsilane as the internal standard.

The number-average molecular weight (M_n) and the weight-average molecular weight (M_w) were determined by gel permeation chromatography (GPC) on a Waters GPC system equipped with a Waters 1515 high performance liquid chromatography (HPLC) pump, a Waters 2414 differential refractometer, and three Styragel columns (HT-3, HT-4, and HT-5) with tetrahydrofuran as the eluent at a flow rate of 1.0 mL/min at 35°C.

The complex viscosity was measured by a TA AR2000 rheometer. The specimen was prepared by the pressing of the B-stage resin into a disc, which was 25 mm in diameter and 1.2 mm in thickness, at room temperature. The parallel-plant fixture was used in oscillation mode with a fixed strain of 0.1% and a fixed angle rate of 10 rad/s to obtain the complex viscosity.

Thermogravimetric analysis was carried out with a TA Q50 thermal analysis system at a heating rate of 20°C/min in the range 50–700°C in an air atmosphere.

A TA Q800 dynamic mechanical analyzer was used to measure the mechanical properties and glass-transition temperature of the QF/TOPI laminates at a heating rate of 5°C/min and a frequency of 1 Hz. Dual-cantilever mode was used. The storage modulus, loss modulus, and tan δ were calculated as factions of temperature.

Thermal mechanical analysis was carried out on TA Q400 thermal mechanical analyzer at a heating rate of 10°C/min in the range 25–300°C with an initial force of 0.02 N, and each sample was scanned twice. The CTEs of samples were calculated according to the second curves. The time to delamination of the QF/TOPI laminates was also conducted by thermal mechanical analysis according to IPC-TM-650; the test was performed by temperature ramping at 10°C/min and was followed by an isothermal process for 1 h to observe the failure.

The tensile properties were examined with an Instron-5567 tensile apparatus according to GB/T 1447–2005 at a test rate of

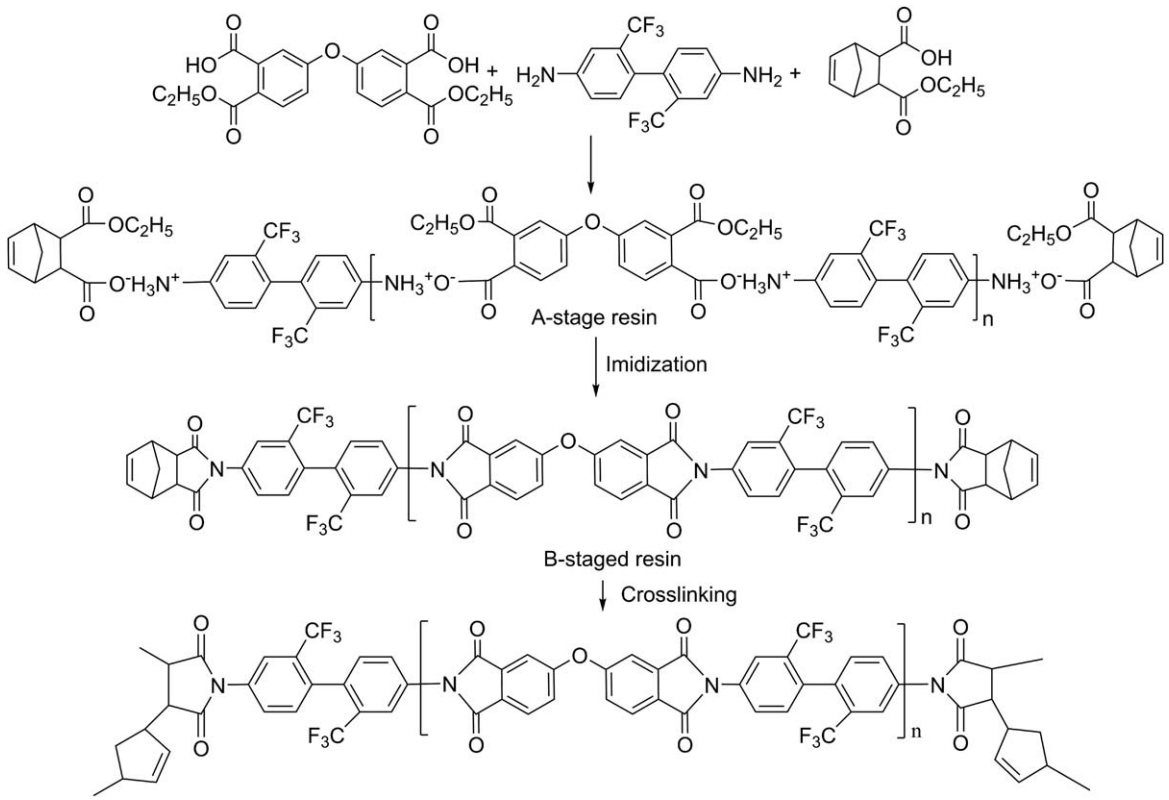

Figure 1. Synthesis of PI.

2.0 mm/min. The flexural strength and modulus of the laminates were obtained according to GB/T 1449–2005, and the test speed was 1.0 mm/min. The peel strength of the Cu/QF/TOPI laminates was tested according to IPC-TM-650. The dielectric properties were characterized by measurement of the microwave dielectric constant and a magnetic permeability measurement system based on a vector network analyzer (Agilent E8363B). The testing frequency ranged from 1 to 12 GHz.

Preparation of the A-Stage Resin Solution

ODPA and NA were esterified separately, and we poured the two ester solutions into the TFDB alcohol solution, where they were cooled to room temperature and then stirred for 8 h under an N_2 atmosphere. As a result, a homogeneous solution was obtained; this was called the A-stage resin solution. In fact, it was a solution mixture of several kinds of salts. The molar ratio of NA to ODPA to TFDB was $2{:}n{:}(n+1)$, and the molecular weight was calculated by eq. (2):

$$M_n = 2M_{NA} + nM_{ODPA} + (n+1)M_{TFDB} - 2(n+1)M_{H2O} \quad (2)$$

where M_n is the theoretical molecular weight of the resin and M_{NA}, M_{ODPA}, M_{TFDB}, and M_{H2O} are the molecular weights of NA, ODPA, TFDB, and H_2O, respectively.

The preparation of the A-stage PI resin solution can be illustrated by the synthesis of TOPI-B as follows. First, ODPA (46.31 g) was esterified in excessive refluxing absolute ethanol (54.94 g) for 2 h to afford the diester derivative (ODPE). Similarly, monoethyl ester of the nadic anhydride (NE) solution was synthesized by the refluxing of a mixture of NA (32.83 g) and absolute ethanol (46.00 g) for 3 h. Then, the ODPE and NE solution were mixed together and added to a solution of TFDB (79.83 g) in anhydrous ethanol (135 g) in a 1000-mL, three-necked flask fitted with a mechanical stirrer, N_2 inlet, and outlet. The monomer mixture was mechanically stirred for 8 h at room temperature to yield a homogeneous A-stage resin solution (TOPI-B, 395 g). The thermosetting PI resins were designed to have different theoretically calculated molecular weights of 1500 g/mol for TOPI-A, 1750 g/mol for TOPI-B, 2000 g/mol for TOPI-C, 2500 g/mol for TOPI-D, and 5000 g/mol for TOPI-E, respectively. The solid concentration of the resin solutions for quartz-cloth impregnation was 37.5 wt %.

B-Stage PI Molding Powders

The A-stage resin solution was evaporated with a rotary evaporator at 60°C to remove most of the solvents. The viscous material obtained was then dried at 60°C for 4–6 h *in vacuo* to give an A-stage solid resin that was light yellow in color. The B-stage PI molding resin was prepared by successive thermal baking of the A-stage solid resin at 120°C for 2 h, 160°C for 1 h, 200°C for 1 h, 220°C for 0.5 h, and 240°C for 0.5 h. It was then pulverized into powder for the following molding process. Meanwhile, the resins were sampled at each imidization temperature for the characterization of FTIR spectroscopy and ^{1}H-NMR to investigate the imidization mechanism.

Preparation of the QF/TOPI Prepregs

The B-quartz-cloth-reinforced PI prepreg (QF/TOPI) was prepared with the following procedure. First, we brushed the A-stage resin solution on the QF cloth and then dried it in air at room temperature. This was followed by a successive thermal

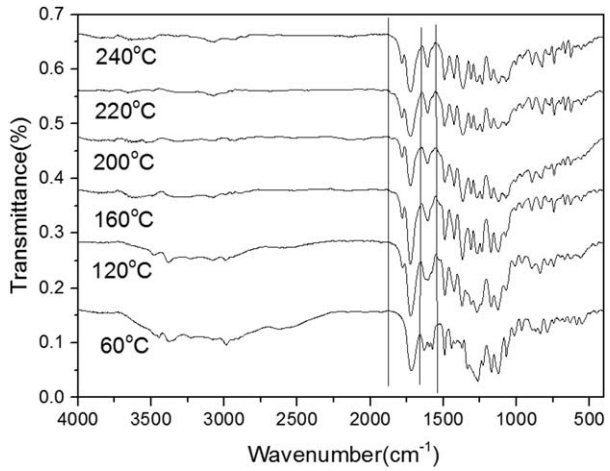

Figure 2. FTIR spectra of the pure resin after treatment at different temperatures.

baking schedule at 160°C for 2 h, 200°C for 1 h, and 220°C for 1 h. The approximate content of resin was obtained by control of the weights of the resin solution and QF cloth.

Fabrication of the QF/TOPI and Cu/QF/TOPI Composite Laminates

The B-stage prepregs were piled up in a mold at room temperature and then placed into a press preheated at 250°C. Then, we heated the press to 280°C. When the press reached 280°C, we applied a pressure of 0.5–2 MPa for 10–20 min, and then, the temperature was increased to 320°C, and the press was subsequently kept at this temperature for 2 h at the given pressure. When the mold was cooled to 50°C, the given pressure was released. The thermosetting QF/TOPI laminate was removed from the mold at room temperature and cut into specimens of the desired size for the thermal, mechanical, and electrical measurements. We prepared the Cu/QF/TOPI composite laminate by putting the Cu foil on the B-stage prepregs and then curing them in the same process as used for the QF/TOPI laminates. The resin contents of the QF/TOPI laminates were obtained according to GB/2577-2005 and were in the range 45–53 wt %.

RESULTS AND DISCUSSION

Preparation and Characterization of the Thermosetting PIs

We prepared thermosetting PI solutions with a solid content of 37.5 wt % in anhydrous alcohol by reacting the ethyl alcohol solutions of NE, ODPE, and TFDB at room temperature by the PMR process according to the PMR method previously reported (Figure 1).[17] The homogeneous resin solutions, with absolute viscosities of 5–15 mPa S at 25°C, showed a golden color and were all stable in both viscosity and color after they were stored for more than 3 months at room temperature (25°C). Structures of the pure resin treated at different temperatures were characterized by the FTIR technique and are shown in Figure 2. The peaks at 3377 and 1572 cm^{-1} were ascribed to the absorption of N—H stretching and in-plane vibrations in nadic acid amide groups, and the peaks at 3446 and 1631 cm^{-1} were attributed to the N—H stretching and in-plane vibrations in 3,3′,4,4′-oxydiphthalic acid amide groups.[19] With increasing treatment temperature, these peaks diminished and then disappeared. At the same time, the peak at 1783 cm^{-1} emerged and became stronger; this peak was due to the vibrations of the imide ring. All of the phenomena showed the currency of thermal imidization. Moreover, the peak at 1272 cm^{-1} was the absorption of the stretching vibration of the ether bond, and the peak at 1597 cm^{-1} represented the stretching vibrations of the carbon–carbon double bond in nadic groups.

Figure 3 shows the ^{1}H-NMR spectrum of the pure resin treated at different temperatures. The A-stage resin baked after 60°C

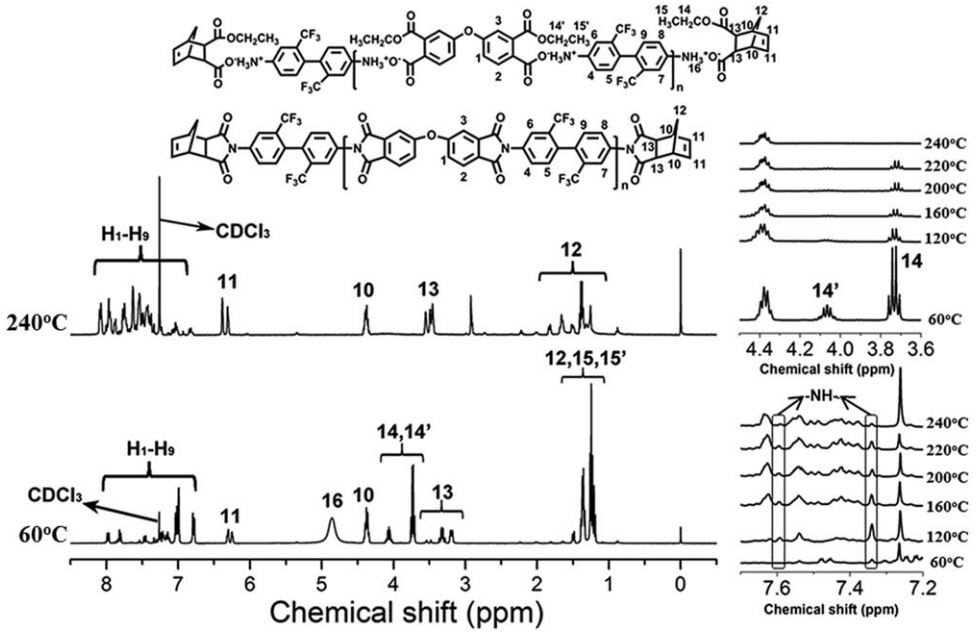

Figure 3. ^{1}H-NMR spectrum of the pure resin after treatment at different temperatures.

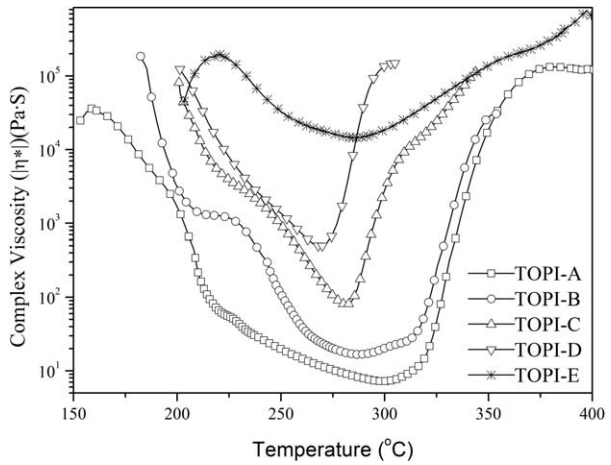

Figure 4. Rheological properties of TOPIs.

was a composite. The main product of the composite was amide salt; this was indicated by the protons observed at a chemical shift of 4.85 ppm ($NH_3^+O^-$).[17,20] After the reactions took place at 120°C for 2 h, the salt changed into polyamide imide; this reaction was proven by the disappearance of the protons at 4.85 ppm and the appearance of protons at 7.34 and 7.59 ppm. The main dealcoholization occurred at 120°C, and the degree of dealcoholization and imidization increased with increasing temperature. This was shown by the decrease in the relatively integral area of peaks at 4.0 and 3.7 ppm (—CH_2—). After it was heated at 240°C for 0.5 h, the resin was fully imidized; this was indicated by the vanishing of the protons at 3.7 ppm and the disappearance of the protons at 7.34 ppm.

GPC was used to investigate the molecular weight of the B-stage PI oligomers. M_n (g/mol) and M_w (g/mol) of B-stage PI resins were 1719 and 4098 for TOPI-A, 1982 and 5042 for TOPI-B, 2052 and 4978 for TOPI-C, 2606 and 6828 for TOPI-D, and 3243 and 8683 for TOPI-E, respectively. The GPC-measured molecular weights were a little larger than the calculated ones for TOPI-A, TOPI-B, TOPI-C, and TOPI-D, but the GPC-measured molecular weight was smaller than the designed molecular weight for TOPI-E. This was attributed to the low reactivity of TFDB.[21] The twisted molecular structure was a disadvantage for the charge transfer in the molecules, and the electron-withdrawing group (—CF_3) decreased the electron density of the anime group (—NH_2). Thus, TFDB had a high reaction activation energy, and it was hard to produce a large-molecular-weight polymer by the PMR method.

Rheological and Mechanical Properties of the B-Stage PIs

Five pure resins were prepared at different calculated molecular weights (M_n) by changes in the content of NA, and the effect of molecular weight on the complex viscosity of the pristine resins was studied. Figure 4 compares the melt viscosity of the B-stage PI resins with different molecular weights at different temperatures. The molten resin viscosities decreased with increasing temperature at the beginning stage and then started to increase after a specific temperature. The first decrease in the molten viscosity was primarily attributed to the melting of the B-stage PI resin, and the following increase in molten viscosity was due to the crosslinking reaction of the nadic endcapping groups. The minimum melt viscosities of these five pure resins rose with increasing molecular weight, and the range of temperature at low viscosity diminished.[22] We concluded that the polymer with a shorter chain length had a larger quantity of endcap groups than the longer ones; thus, it should have taken more time to complete the crosslinking. This may have been the reason why the polymer with a lower molecular weight had more time with a lower viscosity. The smaller molecular weight was attributed to the lower melt viscosity, and the reason was attributed to the fact that the mass center of the molecule could be easily moved when the specimen was heated. However, the movement of larger M_n molecules was harder. In the preparation of the multilayer composite, the lower melt viscosity of the resin was attributed to a high-quality product with little void.

The mechanical properties are another important aspect of a matrix resin. So, the mechanical properties of the pure resins were characterized (Table I) after they were cured at 320°C for 2 h. Because of the high melt viscosity, no high-quality molded plate was obtained for TOPI-E. The tensile modulus and tensile strength increased with increasing molecular weight, and the flexural modulus and strength also had the same tendency. This was attributed to the increasing molecular weight. When the molecular chain got longer, the movement of the molecular chains between the two crosslink points became easier, and under the given stress, the segments could adjust to the change in a shorter time. So, the mechanical properties were better than those in the materials with the same structure but lower molecular weights.

Mechanical Properties of the QF/TOPI Laminate

Because of the rheological properties and mechanical properties, TOPI-B was chosen as the matrix resin for preparing the laminate. The QF/TOPI prepregs were baked up to 220°C to remove the organic volatiles as much as possible before melt processing.

Table I. Mechanical Properties of the Pristine TOPIs with Different Molecular Weights

Specimen	Tensile modulus (GPa)	Tensile strength (MPa)	Elongation (%)	Flexural modulus (GPa)	Flexural strength (MPa)
TOPI-A	1.6	59.5	6.1	3.4	142.5
TOPI-B	1.8	75.2	6.8	3.8	147.1
TOPI-C	2.1	91.1	9.9	3.7	157.4
TOPI-D	2.2	95.7	6.0	4.5	184.8

Table II. Mechanical Properties of the QF/TOPI-B and EG/HTPI-1 Laminates

Specimen	Resin content		Tensile strength (MPa)	Tensile modulus (GPa)	Elongation (%)	Flexural strength (MPa)	Flexural strength (GPa)	Interlaminate strength (MPa)	Impact strength (kJ/m^2)	Peel strength (N/mm)
	wt %	vol %[a]								
QF/TOPI-B-1	-[c]	-[c]	363.9	7.4	6.2	670.8	14.2	61.6	-[c]	-[c]
QF/TOPI-B-2	46	38	567.6	10.1	6.4	845.9	19.5	62.1	141.2	1.06
QF/TOPI-B-3	-[c]	-[c]	557.1	10.8	6.0	835.0	19.5	58.9	146.3	-[c]
QF/TOPI-B-4	53	45	389.5	9.9	7.2	745.8	17.9	60.7	-[c]	-[c]
QF/TOPI-B-5	49	41	547.2	11.4	6.2	834.1	20.0	63.7	-[c]	-[c]
EG/HTPI-1[b]	-	-	270	11.2	4.2	730	24.2	-	53.5	1.23

[a] Estimated from scanning electron microscopy photographs (Figure 5).
[b] Taken from Xu *et al.*'s[1] study.
[c] No test.

The reduction of low-boiling-point volatiles of the B-stage prepregs decreased the odds of voids and defect formation in composite processing. Generally, the PMR-type PI prepregs are treated at temperatures under 200°C to ensure the proper melt viscosity of the B-stage resin.[23,24]

Three different curing temperatures were used: after a curing procedure at 320°C for 2 h, QF/TOPI-B-1 was cured at 320°C for 1 h, QF/TOPI-B-2 was cured at 330°C for 1 h, and QF/TOPI-B-3 was cured at 340°C for 1 h. Then, the mechanical properties of these prepregs were studied (Table II). When the curing temperature was 320°C, the matrix resin could not crosslink sufficiently, so the mechanical properties of QF/TOPI-B-1 were inferior to the mechanical properties of QF/TOPI-B-2 and QF/TOPI-B-3. However, after the higher curing temperature procedure (340°C for 1 h), the matrix resin crosslinked excessively so that the movement of the molecular chains were trapped, and an oxidization layer and microcracks could

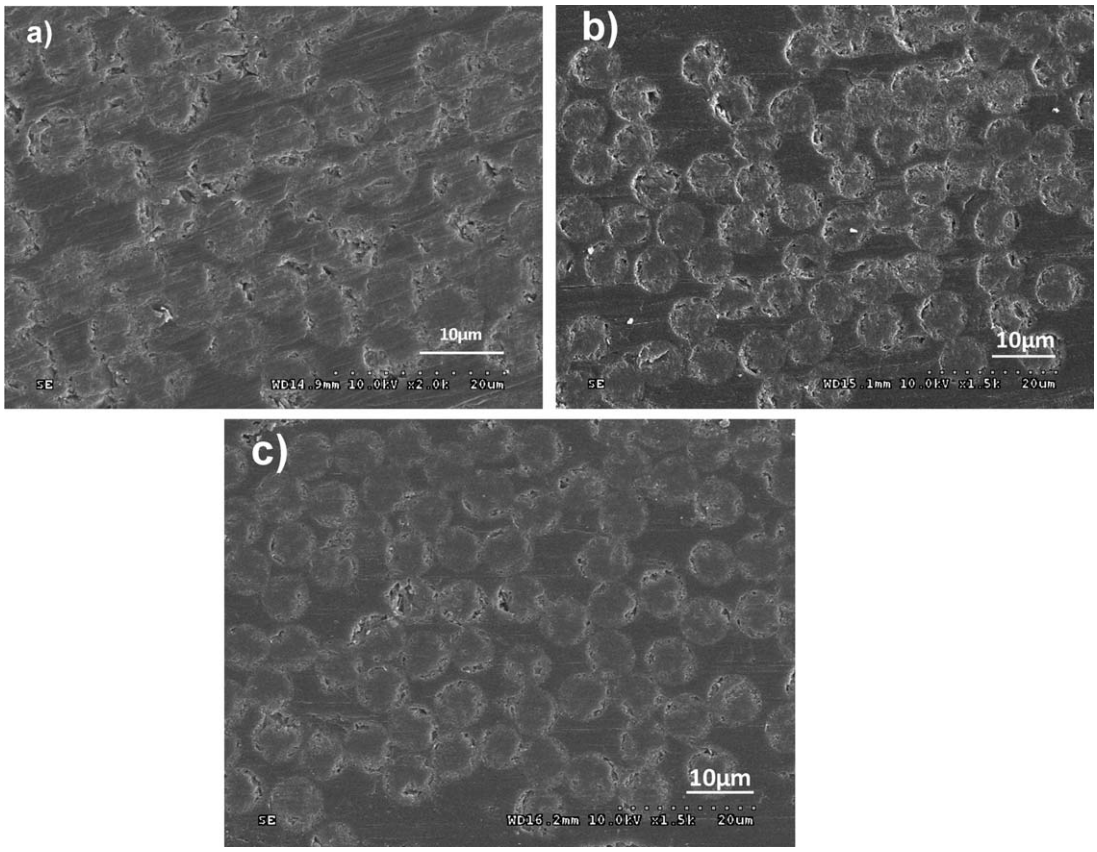

Figure 5. Scanning electron microscopy images of the QF/TOPI-B composite laminates: (a) QF/TOPI-B-4, (b) QF/TOPI-B-5, and (c) QF/TOPI-B-6.

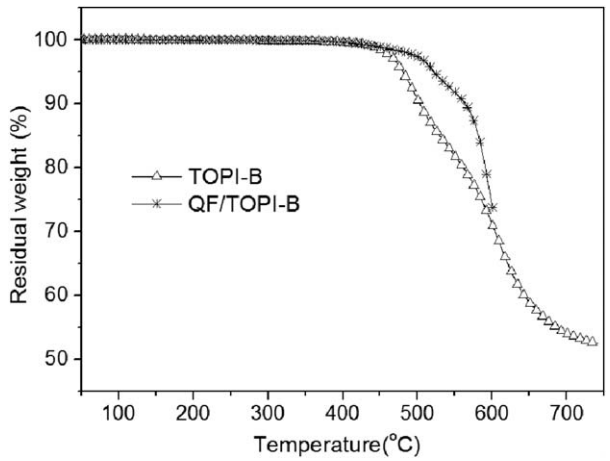

Figure 6. Thermogravimetric analysis curves of the TOPI-B and QF/TOPI-B laminate.

generate on the surface after curing at a harsh temperature. Thus, the properties of the QF/TOPI laminate decreased.[25,26] Therefore, the laminates prepared in the next section were cured at 330°C.

Three QF/TOPI-B prepregs with different matrix resin contents were prepared to investigate the proper resin content of this series of thermosetting PI quartz-fiber-cloth-reinforced laminates. The mechanical properties of this series of laminates were tested (QF/TOPI-B-2, QF/TOPI-B-4, and QF/TOPI-B-5; Table II), and scanning electron microscopy was used to estimate the resin contents in the volumes (Figure 5). The results show that QF/TOPI-B-4, which had the highest resin content, presented a lower mechanical strength compared to QF/TOPI-B-5 and QF/TOPI-B-2. This was attributed to the fact that when the content of quartz-fiber cloth increased, the matrix resin was reinforced well, but when the resin content decreased to a certain limit, the resin could not provide a good adhesion for the interlayer quartz-fiber cloth. On the contrary, when the resin content increased up to a high limit, the PI matrix could not be reinforced sufficiently. Thus, the laminate had a lower tensile strength and modulus.

This study showed that the best curing temperature was 330°C for the QF/TOPI laminate, and the proper resin content was

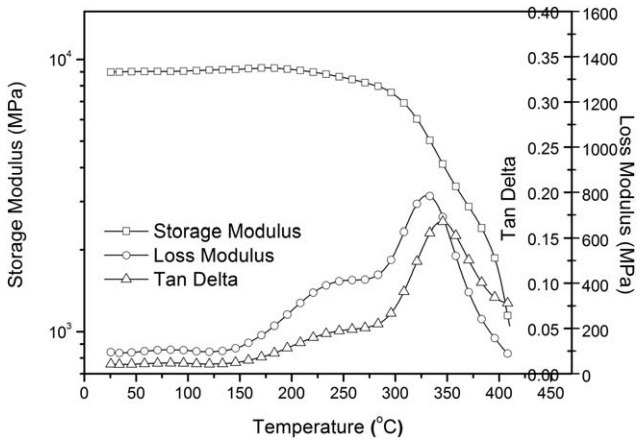

Figure 7. Dynamic mechanical analysis curve of the QF/TOPI-B laminate.

Table III. Thermal Properties of QF/TOPI-B

Specimen	$T_{5\%}$ (°C)[a]	G' (°C)[b]	Tan δ (°C)	CTE (ppm/°C)[c]	
				XY	Z
QF/TOPI-B	500	335	365	8.61	43.04
EG/HTPI-1	488	266	288	11.2	49.7

[a] 5% weight loss temperature.
[b] G', storage modulus onset point.
[c] In the range 50–200°C.

46–49 wt %. TOPI-B was chosen to produce high-quality quartz-fiber cloth composite laminates according the optimized condition mentioned previously, and the mechanical properties of the laminates were studied.

As shown in Table II, the tensile strength of QF/TOPI-2 was 567 MPa, the flexural strength was 845 MPa, the impact strength was 141 kJ/m^2, and the interlaminate strength was 62 MPa. Moreover, the tensile strength was more than 110% higher than that of EG/HTPI-1, the impact strength was more than 160% higher than that of EG/HTPI-1 (53.5 MPa, data obtained from ref. 1), and the flexural strength was more than 15% higher than that of EG/HTPI-1 (730 MPa), but the tensile modulus, flexural modulus, and peel strength were slightly lower than that of EG/HTPI-1. The falling of the flexural modulus may have been due to the fact that HTPI-1 was derived from 3,3′,4,4′-benzophenonetetracarboxylic dianhydride (BTDA). Thus, it had a more rigid molecular chain structure, and the tiny decrease in the peel strength may have been the result of the introduction of F atoms, which decreased the surface energy of PI. Thus, the adhesion properties between PI and the Cu foil deteriorated.[27] Another reason was that the quartz-fiber cloth had better mechanical properties than the E-glass cloth. With the combination of these two reasons, the QF/TOPI composite had better mechanical properties than EG/HTPI-1.

Thermal Properties of the QF/TOPI Composite Laminate

Figure 6 shows the thermogravimetric analysis curve in an air atmosphere (the thermal properties in air conditions well

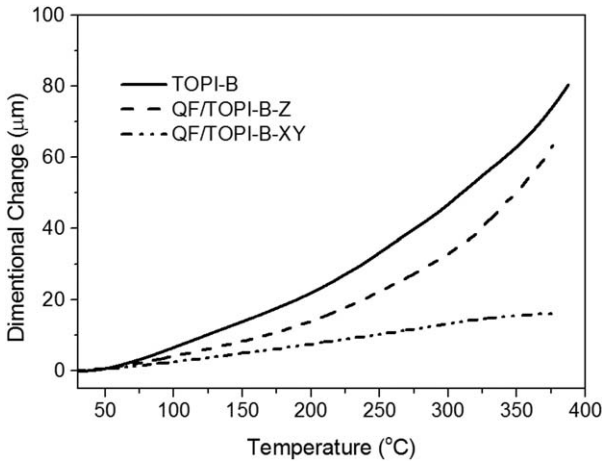

Figure 8. CTE curves of the TOPI-B and QF/TOPI-B in different directions.

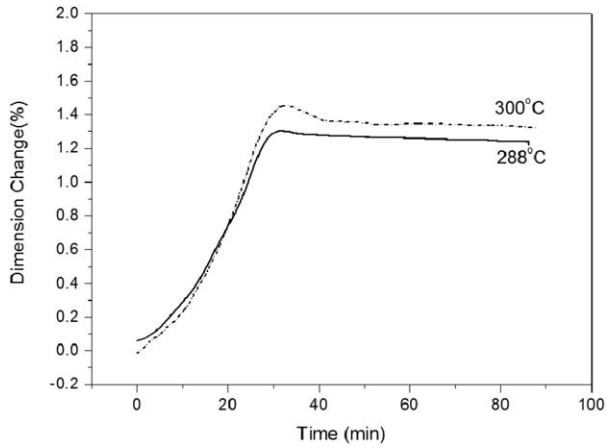

Figure 9. Dimensional changes verse time for QF/TOPI-B at 288 and 300°C.

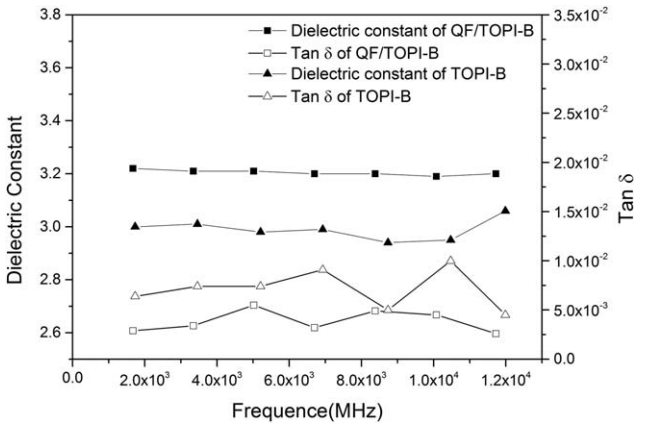

Figure 10. Dielectric constant and dissipation factor of TOPI-B and QF/TOPI-B.

represented the properties in the condition in which the composite laminate was used) of TOPI-B and QF/TOPI. We observed that the QF/TOPI composite laminate with a $T_{5\%}$ higher than 494°C showed a better thermal stability in air than the pure resin TOPI-B. We concluded that the reason was that the quartz-fiber cloth had a better thermal stability. Figure 7 shows a typical dynamic mechanical analysis curve of the QF/TOPI composite laminates. The onset point of the storage modulus was 335°C. This temperature represented the glass-transition temperature of the QF/TOPI-B composite laminate, and the rise of the loss modulus and tan δ between 150 and 270°C was ascribed to the subglass transition of trifluoromethyl.[28,29] The glass-transition temperature of EG/HTPI-1 was 288°C, which was 47°C lower than that of QF/TOPI-B. The increase in the glass-transition temperature of QF/TOPI-B should have been the result of the more rigid molecular structure of TOPI-B.

The thermal properties of the QF/TOPI composite laminate was summarized in Table III. Figure 8 shows the dimensional changes of TOPI-B and QF/TOPI-B in different directions. It presents the effects of the quartz fiber in restricting thermal expansion in a very visible way. The coefficient of thermal expansion of the QF/TOPI composite laminate in a direction parallel to the interlaminate of the quartz cloth (CTE_{XY}) was 8.4 ppm/°C, and the coefficient of thermal expansion in the direction perpendicular to this direction (CTE_Z) for these data was 43.0 ppm/°C. CTE_{XY} was 23% less than that of EG/HTPI-1 11.2 ppm/°C, and CTE_Z was also less than that of EG/HTPI-1 (49.7 ppm/°C). That was because in the *z* direction, the quartz-fiber cloth had a lower expansion coefficient than the pure resin, and in the *xy* direction, the woven quartz fiber restricted the expansion of the composite, so the presence of the quartz fiber lowered the CTE remarkably.

The time to delamination is an important index for a microelectronic packaging substrate. According to IPC-TM-650, the time to delamination can be detected by a thermomechanical analyzer via ramping to a given temperature and isothermal conditions for 60 min to observe whether there is delamination in a specimen. Figure 9 shows the dimensional changes verse time at different temperatures for QF/TOPI-B. Both dimensional changes of QF/TOPI-B at 288°C were lower than those at 300°C; this was due to the fact that the chain movement at 300°C was more active than that at 288°C, so the interchain distance was larger. No delamination took place in the QF/TOPI composite laminate after 60 min of isothermal conditions at 288 and 300°C. This indicated that the QF/TOPI-B composite laminate could endure the tough circumstances of a lead-free microelectronics packaging process in which the temperature would ramp to 260°C. The outstanding thermal resistibility of the QF/TOPI composite laminate promised that it has the potential for use in high-density packaging substrates.

Dielectric Properties of QF/TOPI-B

Table IV shows the electrical and dielectric properties of the QF/TOPI-B composite laminate. QF/TOPI had good electrical insulation, with a surface resistivity of 8.6×10^{15} Ω, a volume resistivity of 1.8×10^{17} Ω cm, a breakdown voltage of 34.9 kV/mm, a dielectric constant of 3.1, and a low water uptake of 0.56%.

Figure 10 shows the dielectric constant and dissipation factor changes of the TOPI-B and QF/TOPI-B composite laminates under different test frequencies. The dielectric constant of QF/TOPI-B was stable in the range 3.17–3.2, although the

Table IV. Electrical and Dielectric Properties of EG/HTPI-1 and QF/TOPI-B

Specimen	Dielectric constant (1 MHz)	Volume resistivity (Ω cm)	Surface resistivity (Ω)	Breakdown voltage (kV/mm)	Water uptake (%)
QF/TOPI-B	3.2	1.8×10^{17}	8.6×10^{15}	34.9	0.5
EG/HTPI-1[a]	4.3	7.7×10^{16}	7.6×10^{16}	28.9	0.6

[a] Taken from Xu *et al.*'s[1] study.

frequency was changing, and these data are slightly higher than those of pure TOPI-B. In contrast, the dissipation factor (tan δ) of TOPI-B was higher than that of QF/TOPI-B, which was in the range 2.3–5.5 $\times$ 10^{-3}. This was attributed to the introduction of F atoms, which lowered the absorption of water, and the presence of —CF_3 groups, which had a large molar volume and could also lower the molecular polarization and then decrease the dielectric constant of the composite, according to the Clas-lius–Mosotti equation mentioned before. In addition, the quartz-fiber cloth had a very high silicon content (>99%), so the dielectric constant of the composite laminate was lowered. Because the quart fiber was an inorganic material, the molecule was more easily polarized than the PI matrix; thus, the dissipation of the QF/TOPI-B was a little higher than that of TOPI-B. The excellent electrical stability indicated that QF/TOPI-B could be applied as a high-frequency, high-speed microelectronic packaging substrate material.

CONCLUSIONS

In this study, we prepared a series of QF/TOPI-B and Cu/QF/TOPI-B composite laminates and studied the resin content of the composite laminates and the curing temperature effects on the mechanical properties of the laminates, and ascertained that the optimal resin content was in the range 46–49 wt % under a curing temperature of 330°C. The composite laminates had excellent mechanical properties with a tensile strength in the range of 567 MPa. The flexural strength was 845 MPa, and the impact strength was 141 KJ/m^2. The QF/TOPI composite laminate also showed such a good thermal stability that the delamination times at 288 and 300°C were both longer than 60 min, the glass-transition temperature was greater than 299°C, and $T_{5\%}$ was greater than 494°C with a low water uptake. In addition to the excellent mechanical properties and thermal stability mentioned previously, the QF/TOPI also exhibited good electrical and dielectric properties, and the dielectric constant was 3.2 at 1 MHz. The breakdown voltage was in range of 34.9 kV/mm. What is more, the dielectric constant and tan δ of the laminate were stable in a wide test frequency in the range of 1–12 GHz; this showed wide prospects for the laminates as applications in IC packaging substrates.

ACKNOWLEDGMENTS

Financial support from the National Key Fundamental Research Development Project (973 Project; contract grant number 2014CB643604), the National Natural Science Foundation of China (contract grant number 51173118), and the Beijing Science & Technology Project (contract grant number D141100003314002) is greatly appreciated.

REFERENCES

1. Xu, H. Y.; Yang, H. X.; Tao, L. M.; Fan, L.; Yang, S. Y. *J. Appl. Polym. Sci.* **2010**, *117*, 1173.
2. Frear, D. In Springer Handbook of Electronic and Photonic Materials; Kasap, S., Capper, P., Eds.; Springer: New York, **2006**.
3. Numata, S. I.; Oohara, S.; Fujisaki, K.; Imaizumi, J. I.; Kinjo, N. *J. Appl. Polym. Sci.* **1986**, *31*, 101.
4. Zhang, Y.-H.; Dang, Z.-M.; Fu, S.-Y.; Xin, J. H.; Deng, J.-G.; Wu, J.; Yang, S.; Li, L.-F.; Yan, Q. *Chem. Phys. Lett.* **2005**, *401*, 553.
5. Tsuchikawa, S.; Arata, M.; Tomioka, K.; Kobayashi, K. Jpn. Pat. JP63159442-A (**1988**).
6. Kennedy, B. W.; Arab, A. U.S. Pat. US3700538-A (**1972**).
7. Mengxian, D. Polyimides: Chemistry, Relationship Between Structure and Properties and Materials; Science: Beijing, **2006**.
8. Matsuura, T.; Ishizawa, M.; Hasuda, Y.; Nishi, S. *Macromolecules* **1992**, *25*, 3540.
9. Hasegawa, M. *High Performance Polym.* **2001**, *13*, S93.
10. Matsuura, T.; Yamada, N.; Nishi, S.; Hasuda, Y. *Macromolecules* **1993**, *26*, 419.
11. Hu, A. J.; Hao, J. Y.; He, T.; Yang, S. Y. *Macromolecules* **1999**, *32*, 8046.
12. Xie, K.; Zhang, S. Y.; Liu, J. G.; He, M. H.; Yang, S. Y. *J. Polym. Sci. Part A: Polym. Chem.* **2001**, *39*, 2581.
13. Kim, S.-U.; Lee, C.; Sundar, S.; Jang, W.; Yang, S.-J.; Han, H. *J. Polym. Sci. Part B: Polym. Phys.* **2004**, *42*, 4303.
14. Chisca, S.; Musteata, V. E.; Sava, I.; Bruma, M. *Eur. Polym. J.* **2011**, *47*, 1186.
15. Fan, B.-H.; Zha, J.-W.; Wang, D.-R.; Zhao, J.; Zhang, Z.-F.; Dang, Z.-M. *Compos. Sci. Technol.* **2013**, *80*, 66.
16. Bhuvana, S.; Saroja Devi, M. *Polym. Compos.* **2007**, *28*, 372.
17. Gao, S. Q.; Wang, X. C.; Hu, A. J.; Zhang, Y. L.; Yang, S. Y. *High Performance Polym.* **2000**, *12*, 405.
18. Lauver, R. W. *J. Polym. Sci. Polym. Chem. Ed.* **1979**, *17*, 2529.
19. Liu, B.; Ji, M.; Fan, L.; Yang, S. Y. *High Performance Polym.* **2013**, *25*, 225.
20. Hu, A. J.; Hao, J. Y.; He, T.; Yang, S. Y. *Macromolecules* **1999**, *32*, 8046.
21. Coburn, J. C.; Soper, P. D.; Auman, B. C. *Macromolecules* **1995**, *28*, 3253.
22. Zhou, J.; Zhang, J.; Liu, W. L.; Ding, M. X.; He, T. B. *J. Mater. Sci.* **1996**, *31*, 5119.
23. Chen, Y.-Y.; Yang, C.-P.; Hsiao, S.-H. *Eur. Polym. J.* **2006**, *42*, 1705.
24. Hao, J. Y.; Hu, A. J.; Yang, S. Y. *High Performance Polym.* **2002**, *14*, 325.
25. Meador, M. A. B.; Lowell, C. E.; Cavano, P. J.; Herrera-Fierro, P. *High Performance Polym.* **1996**, *8*, 363.
26. Safranski, D. L.; Gall, K. *Polymer* **2008**, *49*, 4446.
27. Menezes, M.; Robertson, I. M.; Birnbaum, H. K. *J. Mater. Res.* **1999**, *10*, 4025.
28. Li, F.; Fang, S.; Ge, J. J.; Honigfort, P. S.; Chen, J. C.; Harris, F. W.; Cheng, S. Z. D. *Polymer* **1999**, *40*, 4571.
29. Jacobs, J. D.; Arlen, M. J.; Wang, D. H.; Ounaies, Z.; Berry, R.; Tan, L.-S.; Garrett, P. H.; Vaia, R. A. *Polymer* **2010**, *51*, 3139.